

Abdulhady kadhim

Laser and Optoelectronic Eng.
Dept. University of
Technology, Baghdad, Iraq
abdulhadikadhim5@gmail.com

Received on: 15/07/2017
Accepted on: 13/12/2017
Published online: 07/10/2018

Analytical Characterization and Antimicrobial Activity of Bismuth Nanoparticles Synthesized Using Laser Ablation Technique

Abstract- Bismuth nanoparticles were synthesized using laser ablation technique by focusing solid bismuth target in distilled deionized water by 1064 nm and 532 nm laser radiations generated by Q-switched pulsed Nd:YAG laser, respectively. Synthesized nanoparticles were characterized using UV-Vis spectrophotometer, X-ray diffraction (XRD), Scanning Electron Microscopy (SEM), Transmission Electron Microscopy (TEM), and Atomic Force Microscopy (AFM). The XRD pattern of the synthesized sample was indexed as. UV-Vis spectrophotometer indicated that the peak of absorption spectra of bismuth nanoparticles located in UV-region (230 nm) and increased towards IR region with increase laser energy and laser wavelength. SEM and TEM exhibited spherical shape of bismuth nanoparticles with decrease in particles size with decreasing laser wavelength. The antibacterial activity was tested against *Enterobacter* and *Proteus* (gram-negative bacteria) and *Streptococcus* and *Staphylococcus aureus* (gram-positive bacteria). Synthesized bismuth nanoparticles exhibited inhibitory effect on both bacteria strains with best selectivity against *Enterobacter* and *Proteus* (gram-negative bacteria).

Keywords- Bi NPs, Q-switched pulsed Nd:YAG laser, antimicrobial activity.

How to cite this article: A. kadhim, "Analytical Characterization and Antimicrobial Activity of Bismuth Nanoparticles Synthesized Using Laser Ablation Technique," *Engineering and Technology Journal*, Vol. 36, Part C, No. 1, pp. 71-78, 2018.

1. Introduction

Metallic nanoparticles have inherent and different characterizations compared with their bulk particles due to small particle size, large surface area to volume ratio, shape, distribution, composition, crystallinity and diffusion zones [1-3]. Recently, synthesis, characterizations and applications of mineral NPs have attracted attention. Metallic NPs have unique functional properties such as optical, electrochemical, electronic, magnetic and catalytic due to their geometric factors. Therefore, nanomaterials are used in various applications, such as gas sensors, heterogeneous catalysis, nonlinear optics, microelectronics and medicine [4-6]. Bismuth is a semimetal with many characteristics such as high reflective index, thermoelectric and magnetoresistance behaviors because of low carrier density, high electron mobility, and highly anisotropic Fermi wavelength [7-9]. Bismuth nanoparticles (Bi NPs) have received more attention because of their prospect applications such as thermoelectric cooler, sensor of magnetic field, and power generator. With low toxic effect and high overpotential of hydrogen, Bi film electrodes have recently been utilized in the organic nitrocompounds detection and heavy

<https://doi.org/10.30684/etj.36.1C.11>

2412-0758/University of Technology-Iraq, Baghdad, Iraq

This is an open access article under the CC BY 4.0 license <http://creativecommons.org/licenses/by/4.0>

metal instead of mercury electrodes [7,8]. Bi NPs have been synthesized either by top-down physical methods such as pulsed-laser ablation, dispersion in liquid paraffin, pressure injection, vacuum melting, radio frequency magnetron sputtering, and flash evaporation or by bottom-up chemical methods such as hydrothermal reduction, reduction of ethylene glycol solvothermal, reduction in reverse micelles/microemulsions using NaBH₄, hydrothermal etching, and electrodeposition. Techniques from physics and chemistry have been combined to synthesis of bismuth NPs [10-15]. The laser ablation technique widely has been used for synthesis of nanostructured materials due to its advantages such as fast, absence of any surfactant, pure synthesis method, and extremely high stability for the synthesized NPs under controlled ambient temperature and pressure [16]. Both morphology and composition of the synthesized NPs are related to the applied laser parameters (laser energy, wavelength, repetition rate, pulse width, ablation time, temperature, height of liquid above the surface of target and stabilizing agents) and the target nature and liquid environment, leading to generation of various nanostructures, [17,18]. Furthermore,

biological applications require pure NPs so synthesized NPs using laser ablation are best suited for biological and biochemical applications [19]. The antimicrobial effect of metallic NPs has been ascribed to their little size, and high particular surface region to volume proportion, so NPs penetrate microbes and release metallic ions to permeate microbial membranes [20].

2. Materials and Methods

I. Synthesis of Bi NPs

Bi NPs were integrated utilizing pulsed laser ablation technique. Bismuth plate (1cm × 1 cm × 5mm) was fixed at the bottom of a cylindrical glass vessel filled with 2 mL of double deionized water and focused by Q-switched pulsed Nd:YAG laser as shown in Fig. 1.

The characterization of laser parameters is summarized in Table1. The sample was weighed using very an accurate balance to find the weight percent before and after ablation process.

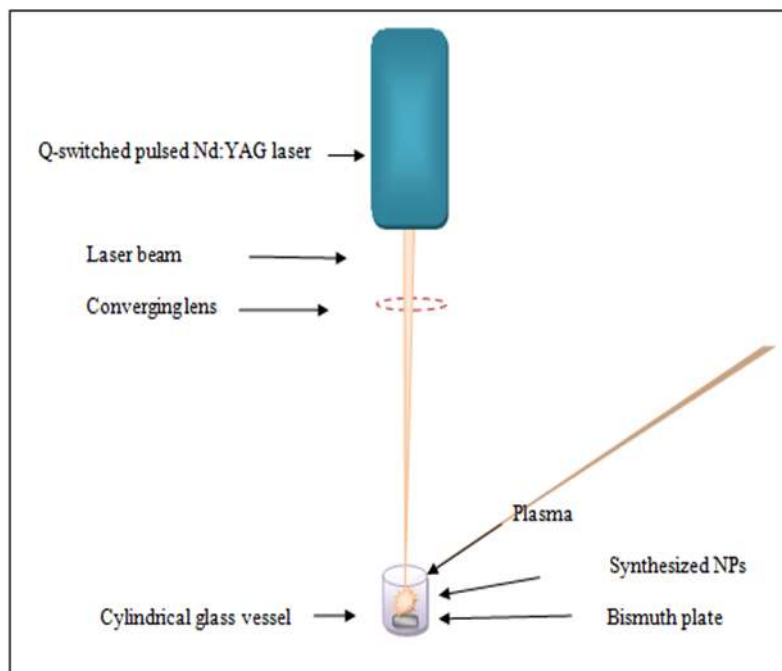


Figure 1: The experimental scheme of Bi NPs synthesized using laser ablation technique

Table 1: The characterization of laser parameters that used in this investigation

Laser parameters	Characterization
Wavelengths	1064 and 532 nm
Laser energy	600-700 mj
Repetition rate	1 Hz
Pulse duration	10 ns
Number of pulses	20 pulse
Focal length	10cm

II. Characterization of Bi NPs

Bi NPs were characterized using optical, structural and morphological advanced techniques. UV-Vis spectrophotometer (Lambda 750, Perkin Elmer) was utilized to determine the assimilation spectra of Bi nanoparticles colloid. X-ray diffraction (XRD) type (Bruker Axs) made in Germany model (D8 Advance) was used to measure the structural properties of Bi NPs, X-ray radiation source was CuK α 1 radiation with

(1.54Å) wavelength at $2\theta = (3^\circ-80^\circ)$. The crystal size was computed via Scherrer equation [13]:

$$D = 0.94 \lambda / \beta \cos \theta \quad (1)$$

Where λ : X-ray wavelength (1.54060 Å), β is the line broadening at half maximum and θ is the diffraction angle.

Scanning Electron Microscopy (SEM), Transmission electron microscope (TEM) and Atomic Force Microscopy (AFM) were used to investigate the morphology and particle size distribution of synthesized Bi NPs.

III. Antimicrobial Effects of Bi nanoparticles

The antibacterial effects of Bi NPs were tested against *Enterobacter*, *Proteus* (gram-negative bacteria), and *Streptococcus*, *Staphylococcus aureus* (gram-positive bacteria) using broth dilution technique. Strains of bacteria were prepared by tubes of 0.5McFarland turbidity standard (5×10^7 cell per mL). The bacterial strains were cultured in nutrient broth. The inhibition rate of bacterial strains was investigated by inoculation of 200 μ L of bacterial suspensions with the broth and various concentrations of Bi NPs (10, 20, 30, 40 and 50) μ g mL⁻¹. Then the tubes were hatched at 37° C for one day. The development of bacteria was tested at 450 nm wavelength and the rate of discouragements were measured as follows [20]: Inhibition rate (%) = $((\text{Control} - \text{test}) / (\text{Control})) \times 100\%$ (2).

3. Results and Discussion

I. Optical properties

UV-Vis spectrophotometer utilized to determine the absorption spectra of bismuth nanoparticles colloidal and the effects of different laser parameters were studied on the optical properties as follows:

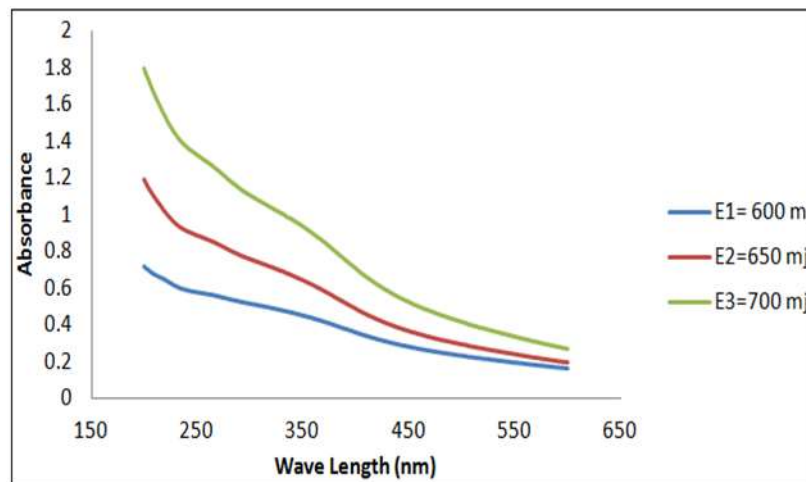


Figure 2: Absorption spectra of Bi NPs colloidal at different laser energy, $\lambda=1064$ nm, 1 Hz, and 30 pulse

Effect of Laser wavelength

Effect of laser wavelength on the synthesized NPs was studied using two wavelengths: fundamental wavelength (1064 nm) and second harmonic generation (532nm) of Q-switched Nd:YAG laser, respectively, as shown in Figure 3. The fundamental wavelength and the second harmonic generation were applied with energy of 700 mJ, 20 pulse and 1 Hz repetition rate. The laser beam was irradiated at the immersed bismuth target in 3mL of DDW. The plasma generated upon the target surface as an ionic region. The brownish colloidal of Bi NPs was obtained when the

Effect of Laser energy

The absorption spectra of the synthesized Bi NPs are shown in Figure 2. The peaks of the absorption spectra in UV region (230) originate due to Surface Plasmon Resonance (SPR) and their sharpness indicates that the synthesized NPs have uniform shape. When a pulse of laser is incident onto the target, the pulse ablates the surface of target then creates an intense plasma, which is limited by liquid media, at the metal-water interface. The laser beam is absorbed by the immersed target leading to rise target thermal energy and causing ionization and vaporization. As a result, the plasma achieves high pressure and temperature. The ionic zone between the water and plasma is active region for chemical reactions between water molecules and bismuth species drive to creation of metal hydroxide NPs, and the later decomposes into metal oxide NPs. It was observed that NPs concentration depend on laser energy where the increase of laser energy leads to increasing in the peak position towards IR region as shown in Figure 2.

number of pulses was increased. The color of solution changed faster when using 1064 nm than that at 532nm. The plasma generated using 1064 nm was higher than that generated by 532 nm due to strong inverse Bremsstrahlung at the IR region so the extracted metal from the metal surface at 1064 nm was higher than that at 532 nm so the ablation efficiency and NPs concentration are

increased at 1064 nm, on the contrary the ablation efficiency and NPs concentration are reduced at the green wavelength (532 nm) due to photo-fragmentation process where the photon energy is absorbed by NPs colloidal [23].

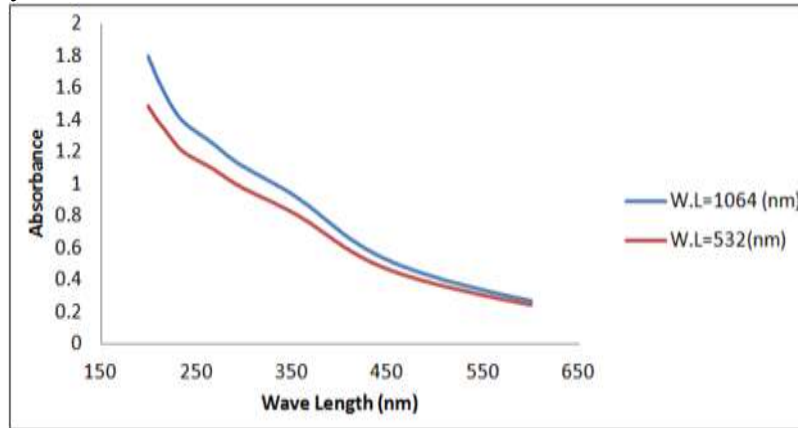


Figure 3: Absorption spectra of Bi NPs colloidal at different laser wavelength, 700 pulse, 1 Hz, and 30 pulse

II. Structural Properties

XRD was used to clarify the Bi nanoparticles phase formation. All the reflections were well indexed to the cubic phase of Bi and can be seen in Figure 4. All XRD parameters of Bi nanoparticles were tabulated in Table 2. The astounding crystallinity and lack of polluting influences can be construed as a result of sharpness and correct number of peaks in the

XRD pattern. Furthermore, it demonstrates that the product is a single phase. The average crystallite size of Bi nanoparticles was found to be 39.4 nm, which was calculated by Scherer's equation.

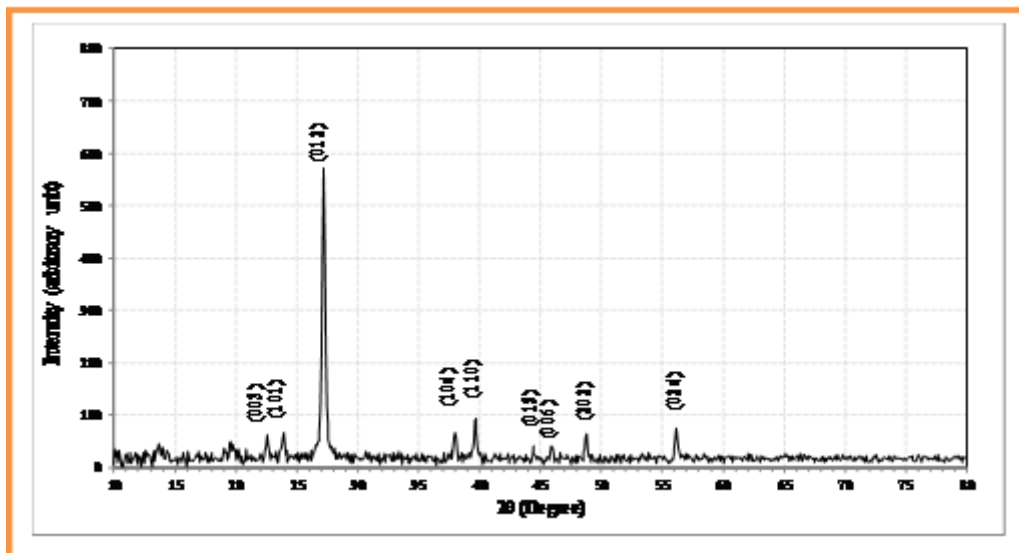


Figure 4: XRD of Bi nanoparticles

Table 2: XRD parameter of Bi nanoparticles

2θ (Deg.)	FWHM (Deg.)	Int%	d _{hkl} Exp.(Å)	G.S (nm)	(hkl)
22.5539	0.2114	8	3.9391	38.3	(003)
23.8751	0.2114	8	3.7240	38.4	(101)
27.2045	0.2378	100	3.2754	34.4	(012)
37.9856	0.2378	9	2.3669	35.3	(104)
39.6503	0.2643	15	2.2713	32.0	(110)
44.4067	0.1586	4	2.0384	54.1	(015)
45.9128	0.1850	5	1.9750	46.7	(006)
48.7402	0.2114	9	1.8668	41.3	(202)
56.1654	0.2642	9	1.6363	34.1	(024)

III. Morphological Properties

Morphology and particle size distribution of Bi NPs synthesized by 1064 nm and 532 nm were characterized using Scanning Electron Microscopy (SEM), Transmission Electron Microscopy (TEM) and Atomic Force Microscopy respectively. The crystalline shape of the synthesized Bi NPs was spherical and the particle size distribution ranged between 20 and

80 nm when using laser wavelength of 1064 nm and between 10 and 60 nm when using laser wavelength of 532 nm as shown in Figure 5 and Figure 6 and Figure 7 respectively.

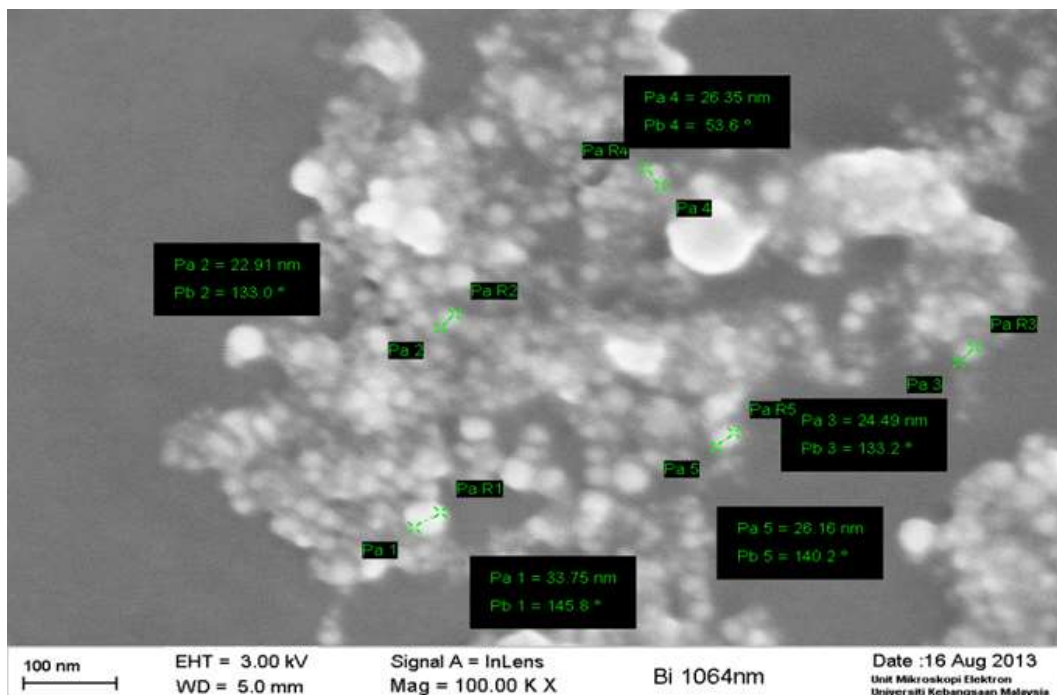


Figure 5: SEM image of Bi NPs synthesized using 1064 nm, 700 mj,1 Hz, 20 pulse

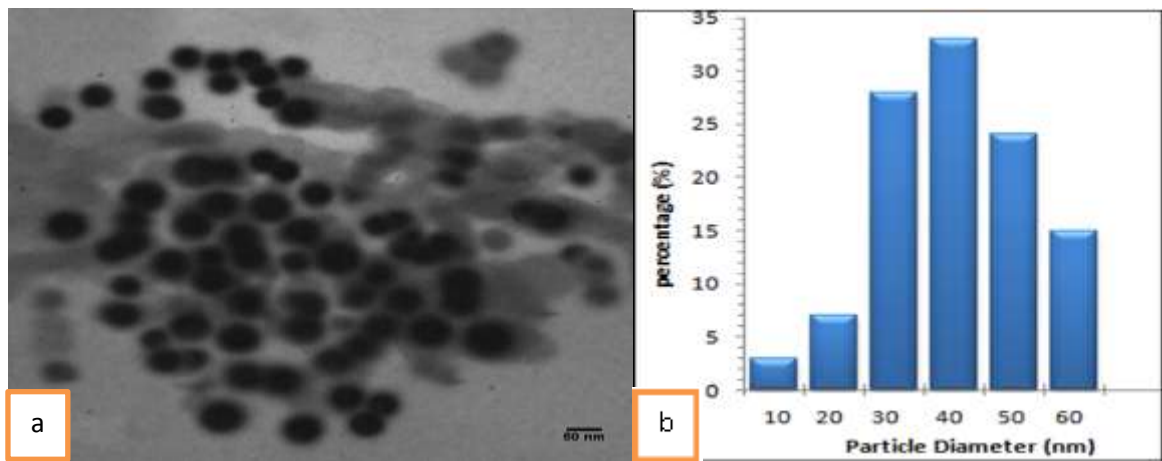


Figure 6: a: TEM image of Bi NPs, b: particle size distribution of Bi Ni Using 532 nm, 700 mj, 1 Hz and 20 pulse

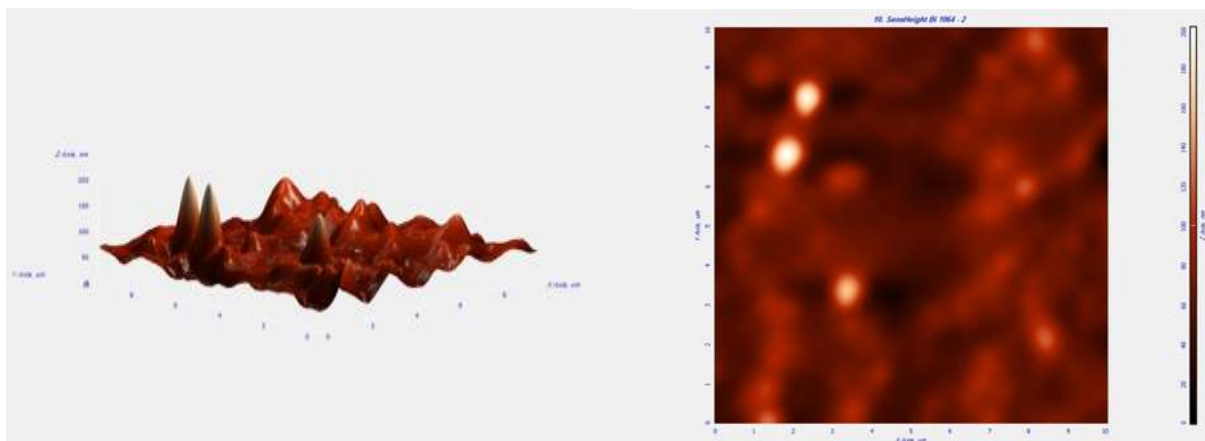


Figure 7: AFM images of 2-D and 3-D surface morphology of Bi NPs Using 1064 nm, 1 Hz, 700 mj and 20 pulse

IV. Antimicrobial activity of Bi NPs

The bacterial optical density was measured using UV-Vis spectrophotometer. Figures 8 and 9 show the optical density of treated pathogenic bacteria (*Enterobacter*, *Proteus*, *S. aureus* and *Streptococcus*) with Bi NPs. The synthesized Bi NPs exhibited antimicrobial activity against bacterial growth.

Distortion occurs in the morphology of bacterial membranes when bacterium is treated to NPs. This causes an increase in membranes permeability, resulting into microorganism killing [24]. Approximately 50 microgram per mL was the optimal concentration of Bi NPs against bacterial growth. The inhibition rate of Bi NPs at the highest concentration (50 microgram per mL) was 48, 46, 45 and 42 % for *Enterobacter*, *Proteus*, *S. aureus* and *Streptococcus*, respectively. From results, the antimicrobial

effects of Bi NPs to inhibit gram-negative bacteria (*Enterobacter*, *Proteus*) were higher than their impact against *S. aureus* and *Streptococcus*. The optimal effect of Bi NPs at the aforementioned concentrations was obtained against *Enterobacter* among all bacterial kinds. Generally, the size of the bacterial cell within limits of micrometer and the outer cellular membranes possess pores within nanometer so the NPs facilely penetrate the membranes of cell [25]. Metallic NPs destroy cell membranes either by generation of reactive oxygen species (ROS) such as superoxide (O_2^-) and hydroxyl (OH^\cdot) radicals or by direct disruption of cell. ROS species oxidize double bonds of phospholipids, driving to membrane fluidity, so the cells more liable to the osmotic stress [26,27].

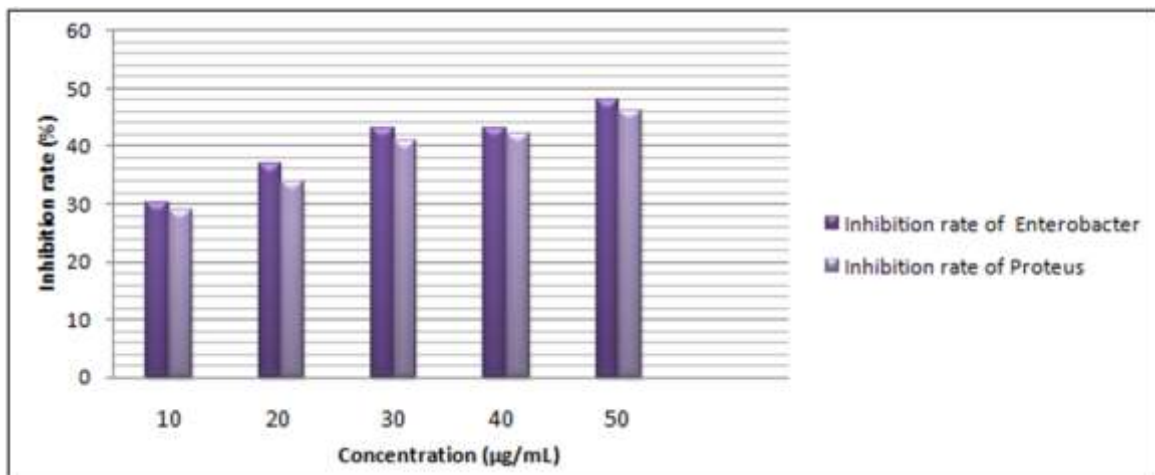


Figure 8: The inhibition rate (%) of treated gram negative bacteria with Bi NPs

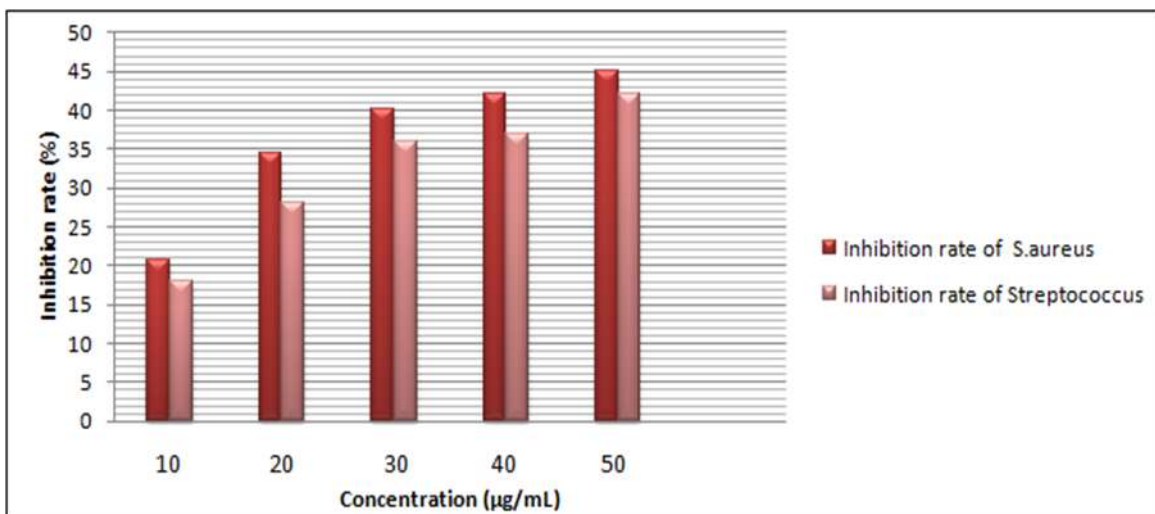


Figure 9: The inhibition rate (%) of treated gram positive bacteria with Bi NPs

4. Conclusion

Bi NPs can be facily generated using laser ablation technique of immersed solid metal in DDDW. UV-Vis absorption spectrum referred that the surface Plasmon resonance of Bi NPs colloidal located at 230 nm. The findings suggest that Bi NPs have significant antibacterial activity against various bacteria strains and more significant effect on the viability of gram-negative bacteria than gram-positive bacteria therefore Bi NPs is suitable for biomedical applications.

References

- [1] S. Dadashi, H. Delavari, R. Poursalehi, "Optical Properties and Colloidal Stability Mechanism of Bismuth Nanoparticles Prepared by Q-Switched Nd:Yag Laser Ablation in Liquid," *Procedia Materials Science*, 11, 679 – 683, 2015.
- [2] S. Prakash Singh and B. Karmakar, "In situ electron beam irradiated rapid growth of bismuth nanoparticles in bismuth-based glass dielectrics at room temperature," *J Nanopart Res.*, 13, 3599–3606, 2011.
- [3] Kh.Z. Brainina, L.G. Galperin, L. Aleksandrovna Piankova, N. Yurievna Stozhko, A. Marksovich Myrzakaev, O. Romanovna Timoshenkova, "Bismuth nanoparticles electrooxidation: theory and experiment," *J Solid State Electrochem*, 15, 2469–2475, 2011.
- [4] R.K. Swarnkar, S.C. Singh, R. Gopal, "Effect of aging on copper nanoparticles synthesized by pulsed laser ablation in water," *Bull. Mater. Sci.* 34, 1363–1369, 2011.
- [5] R.N. Grass and W.J. Stark, "Flame spray synthesis under a non-oxidizing atmosphere: Preparation of metallic bismuth nanoparticles and nanocrystalline bulk bismuth metal," *Journal of Nanoparticle Research*, 729–736, 2006.
- [6] N.V. Tarasenko, V.S. Burakov; A.V Butsen, "Laser ablation plasmas in liquids for fabrication of nanosize particles," *Publ. Astron. Obs. Belgrade* 82, 201–211, 2007.
- [7] X. Chen, S. Chen, W. Huang, J. Zheng, Z. Li, "Facile preparation of Bi nanoparticles by novel cathodic dispersion of bulk bismuth electrodes," *Electrochimica Acta*, 54, 7370–7373, 2009.
- [8] A.H. Al-Hamdani¹, M. Qasim¹, K.S. Rida¹, A. Kadhim "Enhancement of Solar Cell Performance Based On Porous Silicon," *Journal of Nanoscience and Technology*, 2, 2, 73–75, 2016.

- [9] A. Kadhum and H.T. Hussein "Enhancement of the Wear Resistance and Microhardness of Aluminum Alloy by Nd:YAG Laser Treatment," *Scientific World Journal*, Article ID 842062, 5 pages, 2014 .
- [10] K.S. Wu, M.Y. Chern, "Thin Solid Films 516," 3808, 2008.
- [11] X.K. Duan, J.Y. Yang, W. Zhu, X.A. Fan, C.J. Xiao, *Mater. Lett.* 61, 4341, 2007.
- [12] Z.B. Zhang, J.Y. Ying, M.S. Dresselhaus, *J. Mater. Res.* 13, 1745, 1998.
- [13] D.H. Kim, S.H. Lee, J.K. Kim, G.H. Lee, *Appl. Surf. Sci.* 252, 3525, 2006.
- [14] Y.D. Li, J.W. Wang, Z.X. Deng, Y.Y. Wu, X.M. Sun, D.P. Yu, P.D. Yang, *J. Am. Chem. Soc.* 123, 9904, 2001.
- [15] R.K. Swarnkar, S.C. Singh, R. Gopal, "Effect of aging on copper nanoparticles synthesized by pulsed laser ablation in water," *Bull. Mater. Sci.*, 34, 1363–1369, 2011.
- [16] M.T. Le, M. Kovanda, V. Myslik, M. Vrnata, I. Van Driessche, S. Hoste, "Pulsed laser deposition and dip-coating techniques in the fabrication of bismuth molybdate gas sensors," *Thin Solid Films* 497, 2006, 284 – 291.
- [17] E. Yousif, A.A. Al-Amiery, A. Kadhum, A.A.H. Kadhum and A.B. Mohamad, "Photostabilizing Efficiency of PVC in the Presence of Schiff Bases as Photostabilizers," *Molecules*, 20, 19886–19899, 2015.
- [18] K.Y. Niu, J. Yang, S.A. Kulinich, J. Sun, H. Li, X.W. Du, "Morphology control of nanostructures via surface reaction of metal nanodroplets," *J. Am. Chem. Soc.* 132, 9814–9819, 2010.
- [19] N. Acacia, F. Barreca, E. Barletta, D. Spadaro, G. Curro, F. Neria, "Laser ablation synthesis of indium oxide nanoparticles in water," *Appl. Surf. Sci.*, 256, 6918–6922, 2010.
- [20] R.K. Verma, K. Kumar, S.B. Rai, "Near infrared induced optical heating in laser ablated Bi quantum dots," *Journal of Colloid and Interface Science*, 390, 11–16, 2013.
- [21] R. Jeyaraman, J. Kadarkaraihangam, M. Arumugam, R. Govindasamy, A. Abdul, "Synthesis and antimicrobial activity of copper nanoparticles," *Mater. Lett.* 71, 114–116, 2011.
- [22] A. Nath, A. Khare, "Size induced structural modifications in copper oxide nanoparticles synthesized via laser ablation in liquids," *J. Appl. Phys.*, 110, 043111–043116, 2011.
- [23] S.A. Mahdy, Q.J. Raheed, P.T. Kalaichelvan, "Antimicrobial activity of zero-valent iron nanoparticles," *Int. J. Mod. Eng. Res.* 2, 578–581, 2012.
- [24] D. James, B. Harry, R. Jay, M. Astrid, "CO₃O₄ nanoparticle water-oxidation catalysts made by pulsed-laser ablation in liquids," *ACS Catal.* 3, 1–5, 2013.
- [25] SZ. Mortazavi, P. Parvin, A. Reyhani, A. Nozad Golikand and S. Mirershadi, "Effect of Laser Wavelength at IR (1064 nm) and UV (193 nm) on the Structural Formation of Palladium NPs in Deionized Water," *J. Phys. Chem. C*, 115, 12, 5049–5057, 2011.
- [26] I. Sondi, B. Salopek-Sondi, "Silver nanoparticles as antimicrobial agent: a case study on E. coli as a model for gram-negative bacteria," *J. Colloid Interface Sci.* 275, 177–182, 2004.
- [27] S. Jadhav, S. Gaikwad, M. Nimse, A. Rajbhoj, "Copper oxide nanoparticles: synthesis, characterization and their antibacterial activity," *J. Clust. Sci.* 22, 121–129, 2011.
- [28] Y. Chang, M. Zhang, L. Xia, J. Zhang, G. Xing, "The toxic effects and mechanisms of CuO and ZnO nanoparticles," *Materials* 5, 2850–2871, 2012.
- [29] E.T. Salim, M.S. Al Wazny, M.A. Fakhry, "Glancing Angle Reactive Pulsed Laser Deposition (GRPLD) for Bi₂O₃/Si Heterostructure," *Modern Physics Letters B*, 27, 1350122-7- 1350, 2013.